DOI: https://doi.org/10.24425/amm.2026.157793

B. BUĽKO[1], P. DEMETER[1], I. PRIESOL[2], L. FOGARAŠ[1*], S. HUBATKA[1], M. HRUBOVČÁKOVÁ[1], P. ŠMIGURA[1], D. DUBEC[1]

OPTIMIZATION OF CERAMIC REFRACTORY MATERIALS FOR IMPACT PADS IN TUNDISH SYSTEMS FOR CONTINUOUS STEEL CASTING

Increasing demands on cast steel quality and the need to reduce carbon footprint drive the development of new refractory materials. A ceramic composition was developed for spherical tundish impact pads to ensure dimensional stability and resistance to erosion and corrosion. It consists of a thixotropic bauxite mixture with a sol-gel binder and 16% addition of tabular alumina, improving refractoriness and strength. The absence of cement-based binders allows fast, crack-free drying and higher fired strength. Compared to CAC-based castables, it reduces energy consumption and CO_2 emissions. Plant trials confirmed excellent erosion resistance, with no surface deformation or steel penetration, demonstrating full functionality and durability of the pads under molten steel exposure. The material meets technical and environmental requirements, offering a viable alternative for sustainable steel casting operations.

Keywords: Sol-gel bonded refractories; Tundish impact pad; Bauxite castables; Energy efficiency; CO_2 emissions reduction

1. Introduction

An integral part of every continuous steel casting machine is the tundish. Increasing demands for high-quality steel, along with pressure to reduce the carbon footprint of steel production, place growing demands on refractory material manufacturers as well. This results in stringent requirements for tundish systems – not only in terms of optimizing steel flow to ensure steel cleanliness, but also with respect to the performance and application of refractory materials [1,2].

Geometric modifications of the tundish impact zone represent only one aspect of a comprehensive solution in this area. Equally important is the selection of suitable material for the production of the final design of the impact zones. The primary objective was to develop ceramic material that offers good workability during the fabrication of these highly exposed components, while simultaneously exhibiting exceptional resistance to mechanical and fluid dynamic stresses, as well as high resistance to corrosive effects associated with molten steel penetration into the bulk of the material used for the impact pad.

These requirements were defined primarily based on industrial experience, where deformation damage to the shaped impact pads frequently occurs. Such damage often results in a complete loss of functionality or even total destruction of the impact pad during the casting sequence. This, in turn, leads to unbalanced fluid dynamic conditions, particularly toward the end of the casting sequence with direct influence on residence time and inclusions removal potential [3].

In both of the cases mentioned above, there is a simultaneous increase in the presence of macro-inclusions in the cast steel, as well as uneven wear of the working lining of the tundish. At the same time, a key requirement was defined: the developed material must ensure the dimensional stability of the component, as its full functionality depends on the integrity of the spherical (concave) impact surface.

As part of the requirements for the development of a new material for tundish impact zones, ecological considerations regarding the raw materials were emphasized. Additionally, there was a strong demand for minimizing energy consumption associated with the production of the final component – the spherical impact pad – particularly during the drying and thermal processing stages.

2. Materials and methods

Based on the above considerations, the development of the required material was initiated. The primary technological

[1] TECHNICAL UNIVERSITY OF KOŠICE, INSTITUTE OF METALLURGICAL TECHNOLOGIES AND DIGITAL TRANSFORMATION, PARK KOMENSKÉHO 14, 04001 KOŠICE, SLOVAKIA
[2] IPC REFRACTORIES A.S., VSTUPNÝ AREÁL U.S.STEEL 741, 044 54 KOŠICE, SLOVAKIA
* Corresponding author: lukas.fogaras@tuke.sk

requirement was good workability of the material. According to practical experience, this requirement was best met by a thixotropic material [4-6]. Calcined bauxite was selected as the base raw material, as it provides favorable conditions for complete mullitization during thermal preparation prior to the start of casting [7,8].

Its approximate chemical composition and bulk density are shown in TABLE 1. For the choice of binder in the developed refractory material, it was decided to use a proven silicate-based binder employing the sol-gel method. Its basic characteristics are provided in TABLE 2.

TABLE 1

Required Properties of Bauxite

Al_2O_3	91.30 (%)
SiO_2	4.10 (%)
Fe_2O_3	1.10 (%)
TiO_2	2.80 (%)
Density	3.1 ($kg \cdot cm^{-3}$)

TABLE 2

Characteristics of sol-gel binder

Solubility	**Water-miscible**
pH	app. 10
Average particle size	15 (nm)
Specific surface	app. 200 ($m^2 \cdot g^{-1}$)

A key characteristic of refractory materials bonded with sol-gel-based binders is that, after thermal treatment, calcination, and firing, they achieve significantly higher mechanical strength properties. This is due to the absence of hydration reactions typical for CAC systems, which is typical for cement-bonded refractories and involves the presence of CaO – a necessary component of calcium aluminate cements (CAC) used in conventiona hydration reactions typical for CAC systemsl refractory materials [9].

The increased mechanical strength in this case provides a solid foundation for the required resistance to mechanical damage and the negative effects of fluid dynamic forces that can lead to the deformation and structural failure of the impact zone or impact pad.

The second characteristic of refractory materials with sol-gel bonding method is their lower green strength after casting an impact pad into form. However, this limitation is gradually overcome during the drying process, during which water contained in the colloidal silicate binder solution – the sol – and the water used in mixing the concrete batch are removed.

Refractory materials using the sol-gel bonding method-contain no chemically bound or crystalline water. As a result, the drying process of products made from these materials is fast and safe, with no risk of structural damage due to the release of chemically bound water, which typically occurs during the breakdown of hydration reactions typical for CAC systems [10-13].

To enhance both the refractoriness and the strength of the developed material, α-modification of alumina – so-called tabular alumina – was ultimately added at a concentration of 16 weight percent, in the form of a fine powder with a grain size of 0.060 mm [14-15]. This proportion was determined based on a series of tests aimed at achieving stable and guaranteed results of the required properties, essential for serial production.

The material design was based on a bauxite-based sol-gel refractory composition. A comparison of the chemical and physical properties of the original and the newly developed material is shown in TABLE 3. For illustration purposes, data from a bauxite-based refractory material bonded with CAC are also included [9].

TABLE 3

Comparison of Selected Chemical and Physical Properties of Bauxite-Based Refractory Materials

Chemical Composition (%)	**Sol-gel Bonded Bauxite Castables**	**Sol-gel Bonded Bauxite Castables with TA Addition**	**CAC Bonded Bauxite Castables**
Al_2O_3	84.5	88.5	83
SiO_2	8.7	8.3	8.9
Fe_2O_3	1.9	1.2	1.8
CaO	0.3	0.2	1.3
Water demand (%)	2	2	5
Bulk Density ($kg \cdot cm^{-3}$)			
after drying 110°C/24 h	2.890	2.950	2.950
after firing 1400°C/24 h	2.870	2.900	3.000
PLC (%)			
after calcination 500°C/24 h	–0.09	–0.08	0.1
after firing 1200°C/24 h	–15	–0.12	0.5

The final comparison of the strength characteristics of all three castables is shown in Fig. 1. *Tecast BPV CS* represents the base bauxite refractory material with a sol-gel binder. *TECAST BPV CST* is the developed refractory material with a sol-gel binder and an addition of finely ground α-alumina. For comparison, a CAC-bonded bauxite refractory material is also included.

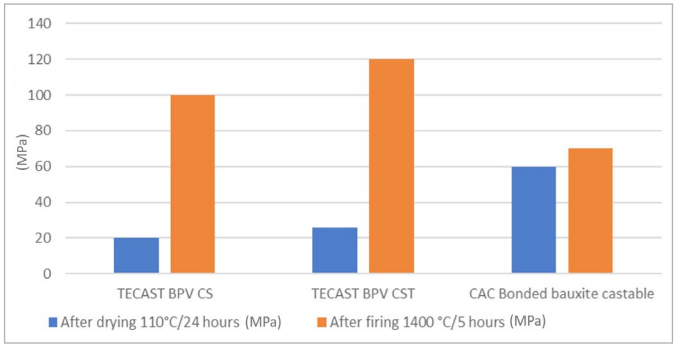

Fig. 1. Comparison of Strength After Drying and After Firing of Individual Refractory Materials

As shown by the displayed values, the developed material exceeds a cold crushing strength (CCS) of 20 MPa after drying, which is more than sufficient to meet the strength requirements for handling and installation under operational conditions. After thermal treatment – firing at 1400°C with a 5-hour hold – the strength of the developed material is nearly twice that of the conventional CAC-bonded bauxite refractory, and approximately 25% higher than that of the bauxite refractory material with sol-gel bonding method.

It should be noted that a sensitive aspect is the so-called green strength of the product, which is defined as the strength after air drying and subsequent demolding. Typical values range between 4-6 MPa and place increased demands on careful handling of the shaped refractory material prior to the actual drying operation [16].

This apparent drawback is partially addressed by the addition of chemical agents that enhance green strength and subsequently degrade during thermal treatment without affecting the mechanical properties of the material. For the purposes of initial testing, a finely ground MgO additive with 99% purity (NEDMAG) was used at a dosage of 0.1 wt.% to increase green strength and accelerate the coagulation of the sol-gel binder.

After the completion of laboratory tests related to material development, the production of prototype impact pads with a spherical surface was initiated, followed by practical testing under plant conditions directly at customer sites.

3. Results and discussion

3.1. Evaluation of the energy demand of production

At this stage, the energy demand associated with the production and processing of impact pads was also evaluated, along with a partial assessment of the carbon footprint of the raw materials. The most energy-intensive components are the binders and the calcined mineral raw materials, whether used as aggregates or as finely ground fractions that form the matrix of the material. In the case of ceramic raw materials, the comparison is neutral, as the same materials are used in both sol-gel bonded and CAC-bonded refractory systems. The key difference lies in the binder systems. When comparing CAC with sol-gel-based binders, the carbon footprint of silicate binders produced via the sol-gel method is significantly lower. Depending on the raw material used for producing silicate sol, this footprint is 30 to 50% lower compared to CAC production [17,18].

The comparison of energy consumption required for drying and thermal treatment of monolithic shaped refractory components made from the developed sol-gel bonded material versus identical shaped parts made from CAC-based refractory materials yielded particularly noteworthy results. The following methodology was used to measure energy consumption: two identical test specimens were placed in a firing furnace and subjected to drying and calcination according to the respective protocols for each type of tested castable. Energy consumption was measured and subsequently converted to an equivalent value of natural gas consumption, which is typically used in industrial operations. The recorded values were recalculated to determine the energy required for drying and thermal processing of shaped refractory products. Heating curves are shown in Fig. 2. The difference in drying and thermal treatment duration between the tested materials is attributed to the nature of their respective bonding systems.

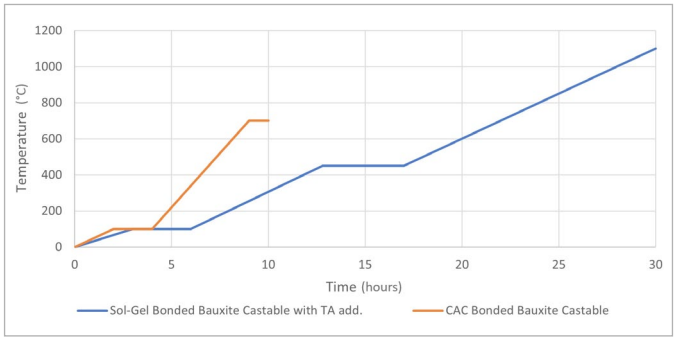

Fig. 2. Description of Drying and Thermal Treatment Curves for the Tested Materials

In the case of CAC-bonded refractory materials, the breakdown of the hydration reactions occurs at approximately 440°C, accompanied by the release of chemically bound water within the system [19]. Therefore, a gradual heating schedule with sufficient holding time is required to safely remove this water. During this phase, the material experiences a decrease in strength due to the degradation of the aforementioned bond. Strength recovery begins only with the onset of sintering at temperatures above 950°C, and the process is completed after reaching 1100°C.

Refractory materials using sol-gel-based binders exhibit a different bonding mechanism. Initially, strength is derived from the gelation of the sol and the formation of a xerogel as free water is removed from the system. This is followed by a gradual increase in strength throughout the entire heating process, without the need for an additional holding stage. The heat treatment can be completed at a temperature of 700°C, at which point the material's strength already approaches the levels typically achieved after full sintering at temperatures above 1000°C.

In addition to energy consumption, CO_2 emissions associated with the energy required for drying and thermal treatment of the components were also a subject of interest. To calculate emissions, the emission factor applicable to natural gas used in our region was applied. Its value is 2.024 kg of CO_2 per 1 m^3 of natural gas. For the reverse calculation of energy consumption into the corresponding amount of natural gas, the calorific value of natural gas was used, which under our conditions is 9.85 kWh per 1 m^3 of natural gas. The measured data are presented in TABLE 4.

The graphical comparison of the measured values is shown in Fig. 3. The energy efficiency – and thus also the economic advantage – of the developed material is clearly evident when compared to conventional CAC-based refractory materials,

TABLE 4

Energy Consumption and CO_2 Emission Values During Drying and Thermal Treatment per 1 kg of Refractory Material Used

	Energy consumption (kWh)	CO_2 production (kg)
Sol-gel Bonded Bauxite Castables with TA Addition	0.516	0.106
CAC Bonded Bauxite Castable	1.22	0.256

while maintaining comparable or improved performance characteristics.

The economic benefit becomes even more significant when the proportional cost of emission allowances is included. This advantage results from both the lower emissions associated with raw material selection (silicate sol versus CAC) and the reduced energy consumption during the drying and thermal preparation of products made from the newly developed material.

It is worth noting that the measured values may not be final, as in serial production of impact pads made from the newly developed material, the reported figures could be even lower due to more efficient energy utilization during the drying and thermal treatment processes.

Based on experience with the installation of sol-gel refractory materials – even in large volumes, such as for tundish linings – it can be stated that the ratios in both energy consumption and CO_2 emissions remain consistent with those presented here [20].

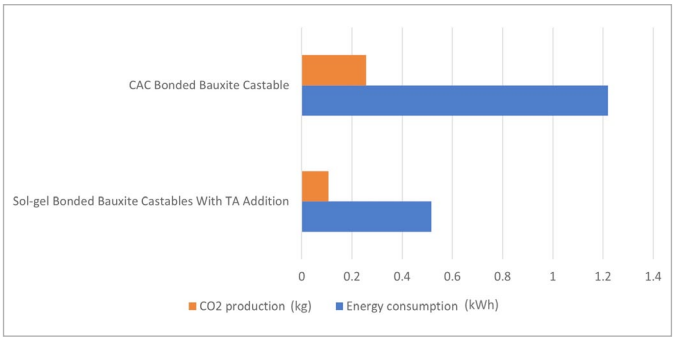

Fig. 3. The comparison of energy consumption and CO2 emissivity for tested materials

To further contextualize the results, it is important to emphasize that the reduction in CO_2 emissions is closely tied not only to lower energy requirements, but also to the fundamental differences in chemical bonding mechanisms. While CAC-bonded systems rely on calcium aluminate hydrates that decompose during firing – releasing chemically bound water and requiring extended thermal profiles – sol-gel bonded systems undergo a phase transformation without such decomposition. This significantly lowers both the thermal load and CO_2 intensity [21]. Moreover, silica sol production processes themselves exhibit lower embedded emissions compared to those of CACs, especially when derived from sodium silicate or ethyl silicate precursors with optimized energy inputs [22].

3.2. Results of Industrial-Scale Testing

Impact pads with a spherical surface were produced from the newly developed material for application in the tundish. The pads were designed to meet the requirements for materials subjected to prolonged exposure to molten steel and the fluid dynamic conditions present at the steel entry point into the tundish. Their shape is shown in Fig. 4.

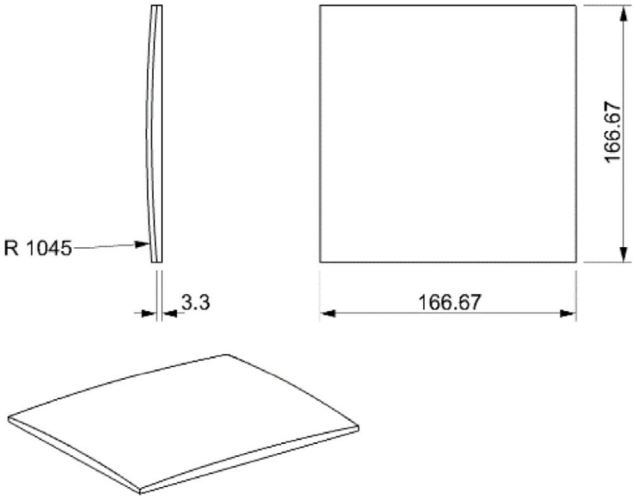

Fig. 4. Shape of the Test Impact Pad

The impact pads were installed in a boat-type tundish, as shown in Fig. 5. The focus of the evaluation was on shape stability and resistance to erosion-related phenomena, including surface deformation of the pad. Additionally, the material underwent post-mortem analysis with special attention given to potential steel-induced corrosion and Fe penetration into the bulk of the material [23,24].

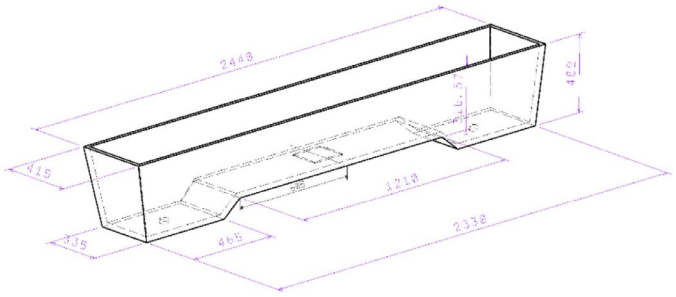

Fig. 5. Boat-Type Tundish

Long casting sequences were performed using the experimental impact pads, with each heat having a volume of 180 tons. The sequences consisted of 28 and 32 heats, respectively. In practice, this means continuous exposure of the impact pads to the dynamic environment of molten steel for 22 to 24 hours. A total of 5,040 and 5,760 tons of steel were cast using the tested pads. The installation of the impact pad is shown in Fig. 6. After the casting was completed and the working lining of the tundish was dismantled, the impact pad was retrieved for evaluation.

Fig. 6 Installing the prototype spherical impact pad in the tundish before casting

The first step was to verify the shape integrity and surface preservation against erosion phenomena. The condition of the impact pad after testing is shown on Fig. 7 and Fig. 8. Based on visual inspection, it was concluded that the pad exhibited no structural damage, and the spherical surface in areas not covered by the slag coating showed no signs of degradation or erosion-induced deformation. To assess the condition of the area covered by the slag layer – which could not be removed – the pad was broken apart to enable evaluation of the impact zone in that section. Even under this type of analysis, no deformation of the spherical surface was observed. It can therefore be concluded that the developed material fully met the requirement for dimensional stability of the impact pad and demonstrated complete resistance to erosion caused by the impingement and subsequent flow of molten steel. Fig. 9 shows the surface condition of the impact pad beneath the slag layer at the point of steel impact, confirming the findings described above.

Fig. 7. Retrieved impact pad after casting, showing preserved shape and minimal surface degradation

Fig. 8. Top view of the impact pad after casting, with no visible deformation and surface coating present

To perform an analysis of potential Fe diffusion from the molten steel into the bulk of the impact pad material, a laser-based elemental quantitative analyzer combined with a Keyence VHX microscope was used. For the analysis, regions located at 2, 4, and 6 cm above the base of the pad were examined. The results of the elemental analysis are shown in Figs. 10 and Fig. 11. Fig. 10 presents the Fe content at 4 cm above the base of the pad, while Fig. 11 shows the results of the quantitative analysis at 6 cm above the base. At a height of 2 cm from the base, no presence of Fe was detected within the bulk of the pad material.

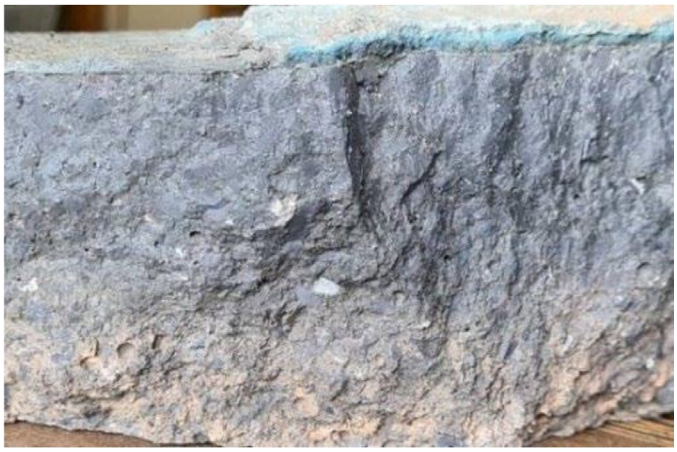

Fig. 9. Surface Condition at the Point of Steel Impact on the Impact Pad

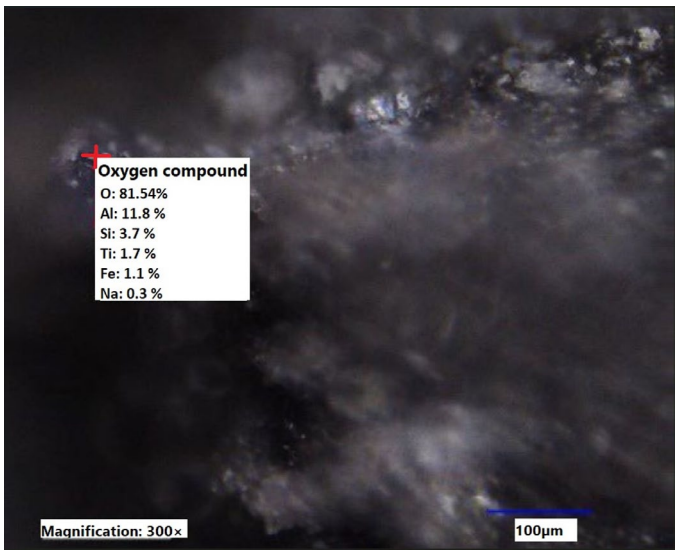

Fig. 10. Fe Analysis at 4 cm Height: 1.1 (% Fe)

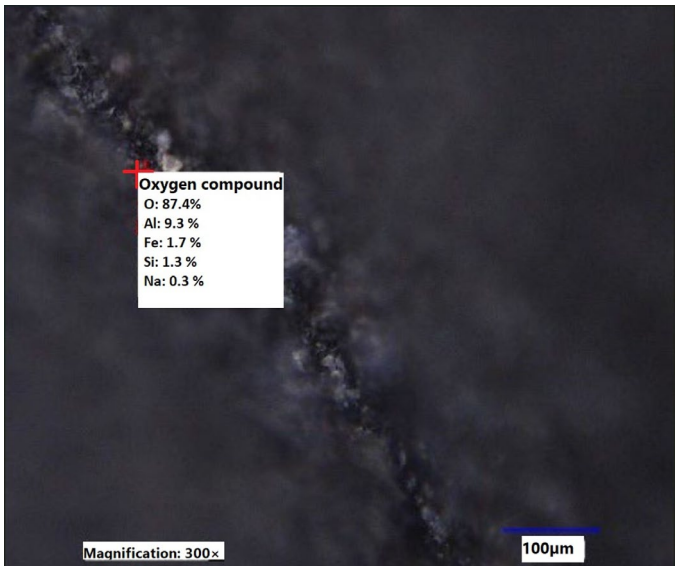

Fig. 11. Fe Analysis at 6 cm Height: 1.7 (% Fe)

No signs of corrosion were observed either macroscopically or microscopically, neither on the spherical surface of the pad nor in the examined sections of the impact pad's material bulk.

4. Conclusion

As part of the research, a new refractory material was successfully developed based on calcined bauxite and a silicate sol-gel binder, enhanced with fine-grained tabular alumina. This material meets the defined objectives – exhibiting high mechanical strength after both drying and firing, increased refractoriness, and resistance to both erosive and corrosive effects of molten steel. Under laboratory conditions, it achieved nearly double the cold crushing strength after firing compared to the reference CAC-bonded castable, while maintaining excellent volumetric stability without significant shrinkage. At the same time, it allows for fast and safe drying without the risk of cracking, simplifying and accelerating the preparation process of shaped components for use. The energy demand for drying and firing components made from this material was experimentally determined to be more than 50% lower than that of conventional cement-bonded materials. This reduction directly translated into proportionally lower CO_2 emissions, contributing to a more environmentally friendly steel production in terms of CO_2 emitted per ton of produced steel.

Prototype impact pads manufactured from this material were successfully tested under real continuous steel casting conditions. During long-term exposure (over 24 hours of uninterrupted casting, equivalent to approximately 5,500 tons of steel), the impact pads maintained their shape and surface integrity. No visible mechanical damage or deformation of the concave surface occurred. Post-mortem analysis revealed only minimal steel penetration into the surface layer (up to 2 mm), indicating the material's high resistance to corrosion and erosion caused by molten steel and slag. The developed material thus demonstrated excellent performance in both laboratory and industrial conditions, representing a promising alternative to conventional cement-bonded castables for tundish system applications. Its use may extend the service life of exposed components while simultaneously reducing energy costs and emissions associated with their production and use.

It can therefore be concluded that the newly developed material fully meets the requirements defined during its development. Its subsequent application in the production of spherical impact pads and their use under real operating conditions fully confirmed this assertion.

Funding

This research work was performed under project APVV-21-0396 and was financially supported by APVV.

REFERENCES

[1] M. Jacoby, Alternative materials could shrink concrete's giant carbon footprint. Chem. Eng. News **98** (45), 26-30 (2020).

[2] D. Tejero Martin, Environmental impact of refractory ceramic coatings: towards low carbon solutions. J. Clean. Prod. **263**, 121144 (2020). DOI: https://doi.org/10.1016/j.jclepro.2020.121144

[3] P. Colombo, Refractory castables: engineering the microstructure. Int. J. Appl. Ceram. Technol. **2** (2), 132-145 (2005). DOI: https://doi.org/10.1111/j.1744-7402.2005.02023.x

[4] Reyma Reotix, Thixotropic behavior of gel bonded refractory concretes. Fire Technology Report, (2023).

[5] U.S. Patent US4212680A, Thixotropic sol gel bonded refractory composition (1980). URL: https://patents.google.com/patent/US4212680A/en

[6] S. Ghosh, Rheological design of low water castables. Mater. Today Proc. **61**, 94-100 (2022). DOI: https://doi.org/10.1016/j.matpr.2022.01.213

[7] J. Li, Formation of mullite–corundum microstructure in bauxite castables. J. Eur. Ceram. Soc. **35** (4), 1121-1128 (2015). DOI: https://doi.org/10.1016/j.jeurceramsoc.2014.11.011

[8] B. Zhao, Microstructure development in high alumina refractory castables. J. Am. Ceram. Soc. **101** (3), 1345-1355 (2018). DOI: https://doi.org/10.1111/jace.15207

[9] T. Neese, Sol–gel bonded castables: high-temperature performance and application potential. Refract. Worldforum **11** (3), 96-101 (2019).

[10] S. Zhang, Nano bonded sol–gel castables: microstructure and mechanical behavior. Ceram. Int. **47** (5), 6841-6850 (2021). DOI: https://doi.org/10.1016/j.ceramint.2020.11.234

[11] X. Xiong, Silica sol bonded refractory castables: performance and mechanism. J. Eur. Ceram. Soc. **31** (8), 1421-1428 (2011). DOI: https://doi.org/10.1016/j.jeurceramsoc.2011.02.013

[12] I. Lancellotti, Microstructure and mechanical performance of sol–gel refractories. J. Non-Cryst. Solids **318** (1), 279-285 (2003). DOI: https://doi.org/10.1016/S0022-3093(02)01459-0

[13] Singh, Akhilesh Kr. Study on the effect of different sols on high alumina castable refractory. 2017. PhD Thesis.

[14] G. Raju, Effect of tabular alumina addition on the strength of bauxite castables. Ceram. Int. **46** (12), 19641-19650 (2020). DOI: https://doi.org/10.1016/j.ceramint.2020.05.279

[15] L. Nevřivová, D. Zemánek, Study of the mineralogical composition of an alumina–silica binder system formed by the sol–gel method. Materials **16**, 15, 5466 (2023). DOI: https://doi.org/10.3390/ma16155466

[16] E. Chudíková, Vlastnosti tvaroviek viazaných sol-gél metódou. In: Zborník REFRACON 2018, Jasná (2018).

[17] Refractories Worldforum, Hydraulic vs. non hydraulic bonding systems in high temperature refractories. Refract. Worldforum **11** (2), 34-40 (2019).

[18] H. Zhao, Energy consumption and emission analysis in ceramic refractory production. Appl. Therm. Eng. **193**, 117060 (2022). DOI: https://doi.org/10.1016/j.applthermaleng.2021.117060

[19] Y. Shinohara, Phase evolution and strength degradation in CAC bonded refractories during firing. J. Am. Ceram. Soc. **100** (10), 4700-4708 (2017). DOI: https://doi.org/10.1111/jace.15025

[20] IntoCast GmbH, Technology brief: Silica sol-gel binding systems in steel ladle applications. Interná technická správa (2023).

[21] L. Sun, D. Ding, G. Xiao, J. Chen, Y. Feng, Cement-free binders in alumina-magnesia refractory castables – A review. High-Temp. Mater. **2**, 10002 (2025). DOI: https://doi.org/10.70322/htm.2025.10002

[22] J.F. Zapata, A. Azevedo, C. Fontes, S.N. Monteiro, H.A. Colorado, Environmental impact and sustainability of calcium aluminate cements. Sustainability **14**, 2751 (2022). DOI: https://doi.org/10.3390/su14052751

[23] X. Liu, Corrosion behavior of bauxite-based castables in steel ladles. Ceram. Int. **47** (10), 14520-14529 (2021). DOI: https://doi.org/10.1016/j.ceramint.2021.01.078

[24] Q. Wang, Post mortem analysis of refractory linings in steel metallurgy. J. Mater. Sci. **55** (5), 2080-2092 (2020). DOI: https://doi.org/10.1007/s10853-019-04128-4